Available online at www.sciencedirect.com
SCIENCE DIRECT®
Chaos, Solitons and Fractals xxx (2006) xxx–xxx
CHAOS SOLITONS & FRACTALS
www.elsevier.com/locate/chaos

Chaos control and synchronization of two neurons exposed to ELF external electric field

Jiang Wang *, Ting Zhang, Yanqiu Che

School of Electrical and Automation Engineering, Tianjin University, Tianjin 300072, China

Accepted 23 March 2006

Abstract

Chaos control and synchronization of two unidirectional coupled neurons exposed to ELF electrical field via nonlinear control technique is investigated. Based on results of space–time characteristics of trans-membrane voltage, the variation of cell trans-membrane voltage exposed to extremely low frequency (ELF) electric field is analyzed. The dynamical behaviors of the modified Hodgkin–Huxley (HH) model are identified under the periodic ELF electric field using both analytical and numerical analysis. Then, using the results of the analysis, a nonlinear feedback linearization control scheme and a modified adaptive control strategy are designed to synchronize the two unidirectional coupled neurons and stabilize the chaotic trajectory of the slave system to desired periodic orbit of the master system. The simulation results demonstrated the efficiency of the proposed algorithms.

1. Introduction

In 1952, Hodgkin and Huxley published four papers [1–4] in series on experiments and models of nerve conduction. Since then, researches on Hodgkin–Huxley (HH) model have been carried out in mainly two ways: One is experiment study, i.e. to obtain data with advanced experimental technologies so as to improve the mathematics form of HH model. The other is mathematical analysis on the model [5]. Because of the character of multi-parameter, strong coupling and nonlinearity, nonlinear theories such as chaos and bifurcation are widely used to perform the analysis. So far, research on the nonlinear dynamical performance of HH model mainly focuses on with the variation of physiological parameters under normal conditions. However, due to wide utilizations of power line and electric equipments, electromagnetic exposure in environment has been nearly one hundred million times stronger than centuries before [6] and many diseases probably caused by electromagnetic exposure are reported [7,8]. Thus the research on HH model exposed to external electric field is of great importance. In this paper, based on results of space–time characteristics of trans-membrane voltage [9,10], the variation of cell trans-membrane voltage exposed to extremely low frequency (ELF) electric field is analyzed. A modified HH model is established by introducing an induced component V_E denoting the effect of external electric field. Then, we analyzed the dynamical behaviors of the modified model under the periodic ELF electrical field.

* Corresponding author. Tel.: +86 22 27402293.
E-mail address: jiangwang@tju.edu.cn (J. Wang).

0960-0779/$ - see front matter © 2006 Elsevier Ltd. All rights reserved.
doi:10.1016/j.chaos.2006.03.098

The researches maybe throw some light on the interference mechanism between biological systems and electromagnetic environment.

On the other hand, chaotic systems are well-known for their extreme sensitivity to small uncertainties in their initial conditions and it has been found that chaos may be useful in many fields such as in a mixing process, or in heat transfer. However, this inherent nonlinear phenomenon is often undesirable in many practical considerations where regular oscillations are needed, like metal cutting processes [11], power electronics [12,13] and so on. In recent years, great efforts have been devoted to controlling and synchronizing chaotic oscillators [14–16]. Several strategies to control chaos have been proposed and investigated with the objective of stabilizing equilibrium points or periodic orbits embedded in chaotic attractors [17–19]. With the development of control theory, various modern control methods, such as adaptive control [20], backstepping design [21,22], active control [23], and time-delay feedback approach [24] have been successfully applied to chaos synchronization in recent years.

The goal of this work is to apply the nonlinear control to synchronizing two unidirectional coupled neurons and converting the chaotic motion of the slave neuron into the periodic orbit as the master neuron. In this work, firstly, we investigated the control strategy using nonlinear feedback linearization. Then, the control scheme comprises an adaptive controller and an uncertainty estimator is proposed. The main idea in dealing with the uncertainties is to lump them into a nonlinear function, in this way the lumping function can be interpreted as a state variable in an extended system. Then, an estimate of the uncertainties is obtained by means of a high-gain estimator. The advantages of the proposed scheme are that it is easier to tune and requires least prior knowledge.

The rest of the paper has been organized as follows. In Section 2, the HH neuronal model is described. The modified HH model exposed to ELF external electric field and the chaos analysis of it is proposed in Sections 3 and 4. The feedback linearization control approach as well as the robust synchronization for the modified model is investigated in Section 5. Finally, the conclusion is drawn in Section 6.

2. HH model

Hodgkin–Huxley equation is a set of four coupled nonlinear differential equations [3]:

$$\begin{cases} \dfrac{dV}{dt} = \dfrac{1}{C_M}[I_{ext} - \bar{g}_{Na} m^3 h (V - V_{Na}) - \bar{g}_K n^4 (V - V_K) - \bar{g}_l (V - V_l)], \\ \dfrac{dy}{dt} = \alpha_y (1 - y) - \beta_y y, \\ y = m, h, n, \end{cases} \tag{1}$$

where V represents trans-membrane voltage in muscle cells and the variables m, h and n represent the sodium activation, the sodium inactivation and the potassium activation, respectively. The external stimulus current can be modeled by the term I_{ext}, usually a tonic or periodic forcing. Since the right parts of the above equations are not function of independent time variable t, the model is a typical autonomous system. $\alpha_y(V)$ and $\beta_y(V)(y = m, h, n)$ are nonlinear functions of V, the equations for them and the nominal values for the system parameters can be found in [3].

The circuit model corresponding to the Hodgkin–Huxley model is represented as Fig. 1.

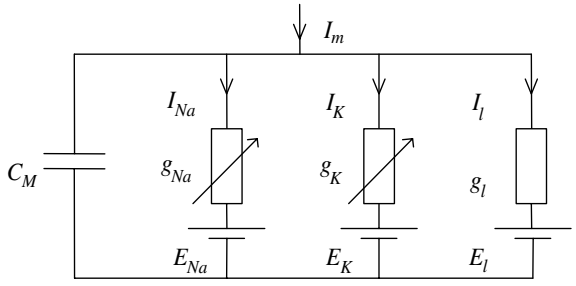

Fig. 1. Original HH circuit model.

3. The modified HH model exposed to ELF external electric field

Due to the accumulation and transportation of ions such as sodium, potassium and chlorine across the membrane, the potential at inner side of membrane is different from that at outer side. Thus an ion trans-membrane voltage V_{ion} is produced, which can be calculated either by the Goldman equation in the rest state or by the HH equation described by (1) in dynamic state.

Since one of main sources of electromagnetic exposure comes from power lines and electric equipments, the interference between biological systems and extremely low frequency (ELF) electric field is intensively studied [5]. Due to the medium characteristic of cell membrane there would produce an induced component V_{E} which is added to the V_{ion} under the effect of ELF electric field. So the overall trans-membrane voltage V_{m} can be expressed as:

$$V_{\text{m}} = V_{\text{ion}} + V_{\text{E}}. \tag{2}$$

Under ELF electric field the capacitance effect of both cytoplasm and outside medium can be neglected because of their large reactance, while the capacitance effect of membrane must be taken into account due to its high resistance.

When exposed to ELF electric field E, the trans-membrane voltage is the sum of ion transportation component V_{ion} and the induced component V_{E}. Then the Hodgkin–Huxley model is modified as the following form:

$$\begin{cases} \dfrac{\mathrm{d}V_{\text{ion}}}{\mathrm{d}t} = \dfrac{1}{C_{\text{M}}}[I_{\text{ext}} - \bar{g}_{\text{Na}} m^3 h(V_{\text{ion}} + V_{\text{E}} - V_{\text{Na}}) - \bar{g}_{\text{K}} n^4 (V_{\text{ion}} + V_{\text{E}} - V_{\text{K}}) - \bar{g}_{\text{l}}(V_{\text{ion}} + V_{\text{E}} - V_{\text{l}})], \\ \dfrac{\mathrm{d}y}{\mathrm{d}t} = \alpha_y(1-y) - \beta_y y, \\ y = m, h, n, \end{cases} \tag{3}$$

The circuit model corresponding to the modified HH model is represented as Fig. 2 [5], which shows that V_{E} behaves as an electromotive force E_{E} added to the membrane.

4. Chaos analysis of the modified HH model

In this section, we will focus on the dynamical behaviors of the modified HH model under the ELF electric field. The purpose of analyzing the modified HH model is to find the different conditions under which the dynamical response of the HH system is chaotic or periodical spiking pattern, and then, the nonlinear control strategies can be applied.

In order to investigate the influence of strength and frequency of the stimulus on the modified HH system, we apply the following method: firstly, keep the strength (or the frequency) invariable, and change the frequency (or the strength) continuously. Then observe the change of the trans-membrane voltage V to get the relationship between the stimulus's frequency (or strength) and the dynamical characters of the potential. To simplify the problem, here, we only analyze the dynamical response to the action of the external electric field V_{E}, i.e. $I_{\text{ext}} = 0$.

The numerical stimulation is chosen as follows:

$$V_{\text{E}} = \frac{A}{2}\sin(\omega t), \tag{4}$$

where the A ($\mu\text{A/cm}^2$) is stimulus strength (peak value), and $\omega = 2\pi f$ (rad/s), f (Hz) is the stimulus frequency.

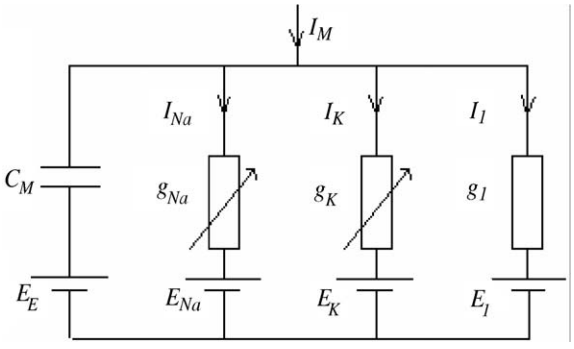

Fig. 2. Modified HH model exposed to ELF electric field.

As stated in Section 1, we should carry out the synchronization control for two individual HH neurons with different initial conditions and parameters. And before the control schemes are applied, the action potential of the two HH neurons should be regular (periodic) and irregular (chaotic), respectively.

Generally speaking, it is difficult to identify the nature of dynamical behavior just from the phase plane. For example, the quasi-periodic states can appear very similar to chaotic states on the phase plane. Therefore, we employ the Lyapunov exponent λ to solve the problem. It is common to refer to the largest one $\lambda_{\max}$, because it determines the predictability of a dynamical system [25]. For a continuous dynamical system, the largest Lyapunov exponent is given by

$$\lambda_{\max} = \lim_{t\to\infty} \frac{1}{t} \log \frac{\eta(t)}{\eta(0)} \tag{5}$$

$\lambda_{\max} < 0$, the orbit attracts to a stable fixed point or stable periodic orbit.
$\lambda_{\max} = 0$, the orbit is a neutral fixed point (or an eventually fixed point).
$\lambda_{\max} > 0$, the orbit is unstable and chaotic. Nearby points, no matter how close, will diverge to any arbitrary separation.

We use the rescaling technique discussed by Wolf et al. [26] for computation of the exponents. This method allows efficient calculation of complete spectrum of the exponents, although it is only the largest exponent which is of interest here.

The parameters of two individual HH neurons:

The first HH neuron:

$$C_{m1} = 1\ \mu F/cm^2,\ g_{K1} = 36\ mS/cm^2,\ g_{Na1} = 120\ mS/cm^2,\ g_{l1} = 0.3\ mS/cm^2,\ V_{K1} = 12\ mV,$$
$$V_{Na1} = -115\ mV \text{ and } V_{l1} = -10.613\ mV.$$

The second one:

$$C_{m2} = 0.9\ \mu F/cm^2,\ g_{K2} = 32.4\ mS/cm^2,\ g_{Na2} = 108\ mS/cm^2,\ g_{l2} = 0.27\ mS/cm^2,$$
$$V_{K2} = 10.8\ mV,\ V_{Na2} = -103.5\ mV,\ V_{l2} = -9.5517\ mV.$$

Initial conditions are chosen as:

$$x_{1,0} = (0.00002\ mV,\ 0.05293\ mV,\ 0.59612\ mV,\ 0.31768\ mV) \text{ and } x_{2,0} = (0,0,0,0).$$

The spiking patterns of voltage and the V–m phase plane diagram in the first neuron are shown in Figs. 3 and 4, respectively, when the amplitude and frequency parameter of the stimulation is specified as: $V_{E1} = 5\sin(2\pi \times 40t/1000)$, and the dynamical behavior of the individual neuron is regular (periodic), which can be demonstrated by the analysis of the Lyapunov exponent λ in Fig. 5. Then, when $V_{E2} = 5\sin(2\pi \times 110t/1000)$, the individual neuron is chaotic, as shown in Figs. 6 and 7, and the Lyapunov exponent λ is analyzed in Fig. 8.

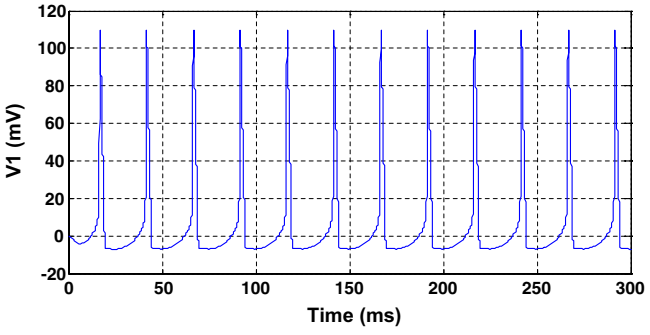

Fig. 3. Regular (periodic) spiking patterns of voltage in the first HH neuron.

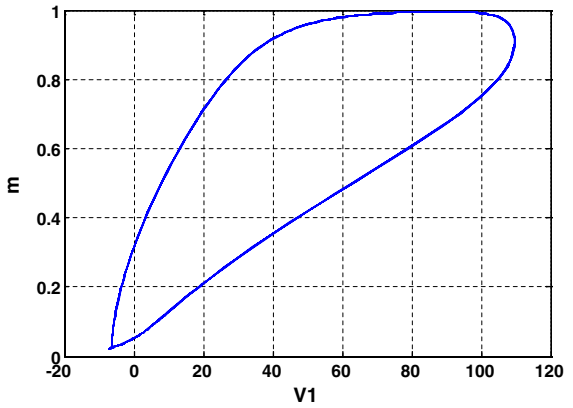

Fig. 4. *V–m* phase plane diagram in the first system.

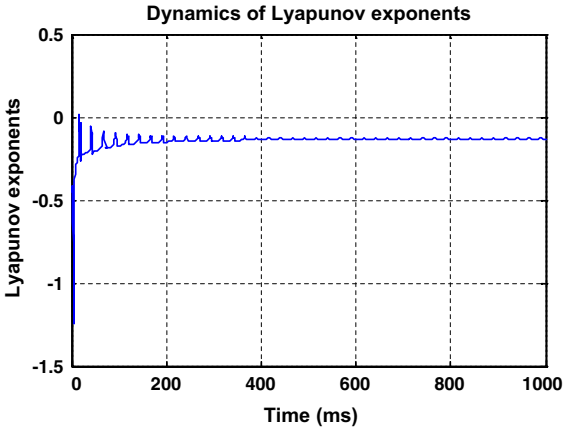

Fig. 5. The largest Lyapunov exponents λ_{max} of the first HH neuron in Fig. 3.

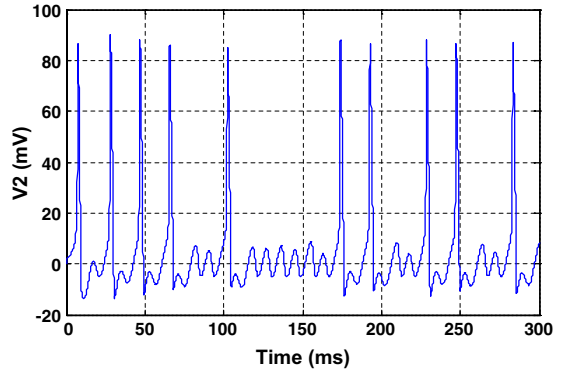

Fig. 6. Irregular (chaotic) spiking patterns of voltage in the second HH neuron.

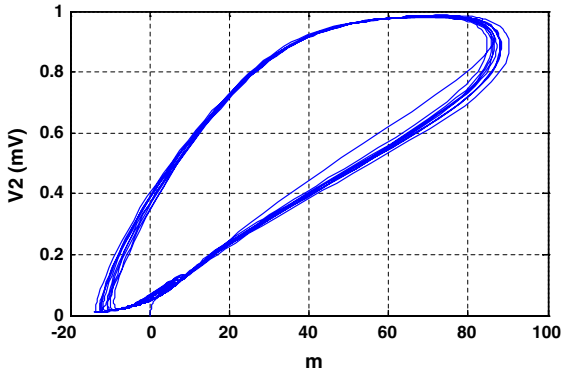

Fig. 7. V–m phase plane diagram in the second system.

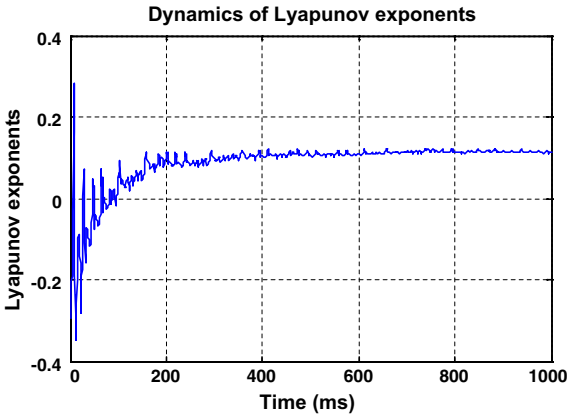

Fig. 8. The largest Lyapunov exponents $\lambda_{\max}$ of the second HH neuron in Fig. 6

5. Synchronize HH system using nonlinear control design

5.1. Description of the HH system based on the modified HH model

In order to state the synchronization problem of two HH neurons, let us redefine the HH system of equations based on the modified HH model which has been stated in Section 3.

$$\begin{cases} \dot{x}_{1,\mathrm{M}} = \frac{1}{C_{\mathrm{mM}}}[I_{\mathrm{extM}} - \bar{g}_{\mathrm{NaM}} x_{2,\mathrm{M}}^3 h(x_{1,\mathrm{M}} - V_{\mathrm{NaM}} + V_{\mathrm{EM}}) - \bar{g}_{\mathrm{K}} x_{4,\mathrm{M}}^4 (V - V_{\mathrm{KM}} + V_{\mathrm{EM}}) - \bar{g}_{\mathrm{lM}}(x_{1,\mathrm{M}} - V_{\mathrm{lM}} + V_{\mathrm{EM}})], \\ \dot{x}_{i,\mathrm{M}} = \alpha_y(x_{1,\mathrm{M}})(1 - x_{i,\mathrm{M}}) - \beta_y(x_{1,\mathrm{M}}) x_{i,\mathrm{M}}, \\ y = m, h, n, \quad i = 2, 3, 4, \end{cases} \tag{6}$$

$$\begin{cases} \dot{x}_{1,\mathrm{S}} = \frac{1}{C_{\mathrm{mS}}}[I_{\mathrm{extS}} - \bar{g}_{\mathrm{NaS}} x_{2,\mathrm{S}}^3 h(x_{1,\mathrm{S}} - V_{\mathrm{NaS}} + V_{\mathrm{ES}}) - \bar{g}_{\mathrm{K}} x_{4,\mathrm{S}}^4 (V - V_{\mathrm{KS}} + V_{\mathrm{ES}}) - \bar{g}_{\mathrm{lS}}(x_{1,\mathrm{S}} - V_{\mathrm{lS}} + V_{\mathrm{ES}})] + u, \\ \dot{x}_{i,\mathrm{S}} = \alpha_y(x_{1,\mathrm{S}})(1 - x_{i,\mathrm{S}}) - \beta_y(x_{1,\mathrm{S}}) x_{i,\mathrm{S}}, \\ y = m, h, n, \quad i = 2, 3, 4, \end{cases} \tag{7}$$

where the state vector $x_{i,\mathrm{M}}$ and $x_{i,\mathrm{S}}$ ($i = 1, 2, 3, 4$ and subscripts M, S stand for the master and slave system, respectively) are the four variables V, n, m and h in each system. The added term u in (7) is the control force (synchronization command). The system (6) is the so-called "master" system, whereas the system (7) represents the "slave" system.

5.2. Feedback linearization of nonlinear systems

The synchronization problem can be seen as follows: let us define $x \in \mathbb{R}^n$ such that $x_i = x_{i,\mathrm{M}} - x_{i,\mathrm{S}}$, for $i = 1, 2, 3, \ldots, n$. Then, the following dynamical system describes the dynamics of the synchronization error [18,27]:

$$\dot{x} = \Delta F(x, p_1) + \Delta T(t, p_2) - Bu = \Delta f(x) + \Delta I(t) - Bu, \quad y = h(x) = x_1, \tag{8}$$

where $\Delta f(x)$ is a smooth vector field, $\Delta I(t)$ is the difference between the external exciting forces and $y \in \mathbb{R}$ represents the measured state of the system. In this way, the synchronization problem can be considered as the stabilization of Eq. (8) at the origin. In other words, the problem is to find a feedback control law $u = u(t)$ such that $\lim_{t\to 0} x \to 0$ (which implies that $x_{\mathrm{S}} \to x_{\mathrm{M}}$) as $t \to \infty$. Then, according to the definition in [28], the HH systems are exactly synchronization.

Now, let us consider the following stabilizing control law [29],

$$u = \frac{1}{L_{\mathrm{g}} L_{\mathrm{f}}^{\rho-1} h(x)} \left(-L_{\mathrm{f}}^{\rho} h(x) - c_0 h(x) - c_1 L_{\mathrm{f}} h(x) - \cdots - c_{\rho-1} L_{\mathrm{f}}^{\rho-1} h(x) \right), \tag{9}$$

where $L_{\mathrm{f}} h(x)$ stands for the Lie derivative of the function $h(x)$ along the vector field f, and the constant parameters $c_0, c_1, \ldots, c_{\rho-1}$, belong to the polynomial $p(s) = c_0 + c_1 s + c_{\rho-1} s^{\rho-1} + s^{\rho}$, of which all the eigenvalues have negative real part. It can be easily shown that the relative degree for the system (8) is $\rho = 1$.Then, the system (8) is stabilized by the control law $u = [-L_{\mathrm{f}} h(x) - C_0 h(x)]/L_{\mathrm{g}} h(x)$, and C_0 is a positive real constant that represents the convergence rate which can be interpreted as a synaptic like control current [18]. Then, we obtain the control action:

$$\begin{aligned} u = {} & \frac{1}{C_{\mathrm{mM}}} [I_{\mathrm{extM}} - \bar{g}_{\mathrm{NaM}} x_{2,\mathrm{M}}^3 h(x_{1,\mathrm{M}} - V_{\mathrm{NaM}} + V_{\mathrm{ES}}) - \bar{g}_{\mathrm{K}} x_{4,\mathrm{K}}^4 (V - V_{\mathrm{KM}} + V_{\mathrm{ES}}) - \bar{g}_{\mathrm{lM}} (x_{1,\mathrm{M}} - V_{\mathrm{lM}} + V_{\mathrm{ES}})] \\ & - \frac{1}{C_{mS}} [I_{\mathrm{extS}} - \bar{g}_{\mathrm{NaS}} x_{2,\mathrm{S}}^3 h(x_{1,\mathrm{S}} - V_{\mathrm{NaS}} + V_{\mathrm{ES}}) - \bar{g}_{\mathrm{K}} x_{4,\mathrm{S}}^4 (V - V_{\mathrm{KS}} + V_{\mathrm{ES}}) - \bar{g}_{\mathrm{lS}} (x_{1,\mathrm{S}} - V_{\mathrm{lS}} + V_{\mathrm{ES}})] + C_0 (x_{1,\mathrm{M}} - x_{1,\mathrm{S}}). \end{aligned} \tag{10}$$

Implementing the control action (10) into (7) lead to the following set of coupled nonlinear differential equations:

$$\begin{cases} \dot{x}_{1,\mathrm{M}} = \frac{1}{C_{\mathrm{mM}}} [I_{\mathrm{extM}} - \bar{g}_{\mathrm{NaM}} x_{2,\mathrm{M}}^3 h(x_{1,\mathrm{M}} - V_{\mathrm{NaM}} + V_{\mathrm{EM}}) - \bar{g}_{\mathrm{K}} x_{4,\mathrm{M}}^4 (V - V_{\mathrm{KM}} + V_{\mathrm{EM}}) \\ \qquad -\bar{g}_{\mathrm{lM}} (x_{1,\mathrm{M}} - V_{\mathrm{lM}} + V_{\mathrm{EM}})], \\ \dot{x}_{i,M} = \alpha_y (x_{1,\mathrm{M}})(1 - x_{i,M}) - \beta_y (x_{1,\mathrm{M}}) x_{i,M}, \\ \dot{x}_{1,\mathrm{S}} = \frac{1}{C_{\mathrm{mM}}} [I_{\mathrm{extM}} - \bar{g}_{\mathrm{NaM}} x_{2,\mathrm{M}}^3 h(x_{1,\mathrm{M}} - V_{\mathrm{NaM}} + V_{\mathrm{EM}}) - \bar{g}_{\mathrm{K}} x_{4,\mathrm{M}}^4 (V - V_{\mathrm{KM}} + V_{\mathrm{EM}}) \\ \qquad -\bar{g}_{\mathrm{lM}} (x_{1,\mathrm{M}} - V_{\mathrm{lM}} + V_{\mathrm{EM}})] + C_0 (x_{1,\mathrm{M}} - x_{1,\mathrm{S}}), \\ \dot{x}_{i,\mathrm{S}} = \alpha_y (x_{1,\mathrm{S}})(1 - x_{i,\mathrm{S}}) - \beta_y (x_{1,\mathrm{S}}) x_{i,\mathrm{S}}, \end{cases} \tag{11}$$

$$y = m, h, n; \quad i = 2, 3, 4.$$

The next step is carrying out numerical simulations for the above HH synchronization system (11). And now we can use the results of Section 4, choosing the first HH neuron as the master system and the second neuron as the slave system. All the stimulations, the parameters and the initial conditions are the same as them in Section 4. The control action was implemented at time $t_0 = 180$ ms, and $C_0 = 0.5$ which leads to rapid synchronization. In Fig. 9, the initial state of the master (solid line) and the slave (dashed line) systems is periodic and chaotic, respectively. After the controller (10) is applied, the slave system transform from chaotic state into periodic orbit synchronizing with the master one. In Fig. 10, the synchronization error converges to zero after the controller (10) is applied, and Fig. 11 is the $V_{\mathrm{M}} - V_{\mathrm{S}}$ phase plane diagram of system (11), which shows the exactly synchronization.

5.3. Robust synchronization

The feedback linearization control which has been carried out in Section 5.2 requires information about currents flowing through the membrane and the ionic channels activation and inactivation variables for the master and slave systems. Such a coupling cannot be implemented in practice on real neurons. Hence, the feedback (10) must be modified. In what follows, an adaptive scheme to yield robust synchronization is realized.

The synchronization error system (8) can be globally transformed into the following canonical form [29]:

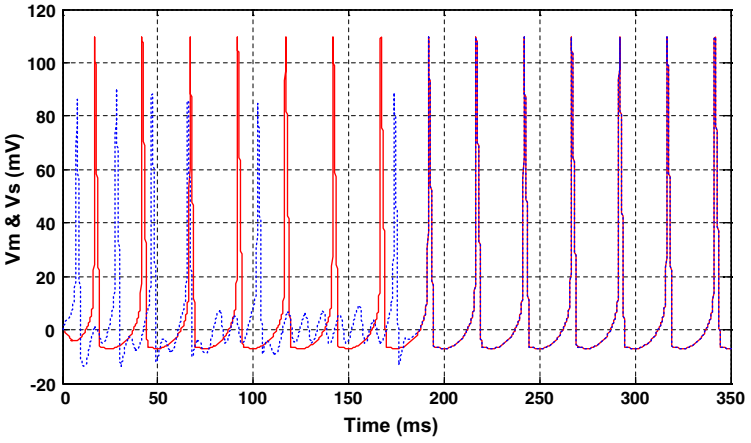

Fig. 9. Regular synchronized state of the action potentials under feedback linearization control (10).

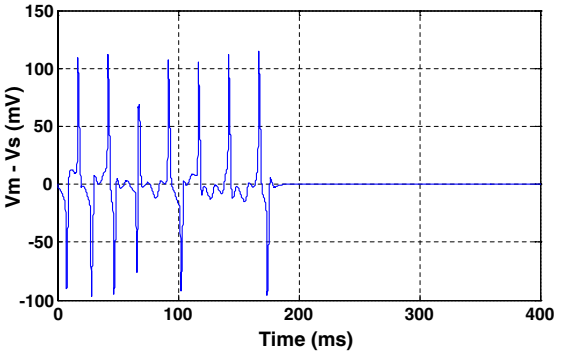

Fig. 10. Synchronization error of system (11).

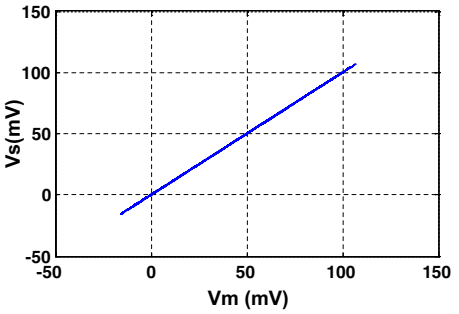

Fig. 11. Phase plane diagram of system (11).

$$\begin{cases} \dot{z}_i = z_{i+1}, \quad i = 1, \ldots, \rho - 1 \\ \dot{z}_1 = \delta(z, t) + u, \\ y = z_1, \end{cases} \tag{12}$$

where $\delta(z,t) = L_f^\rho h(x)$ and $y = z_1$ is the output of the uncertain system. Since $f(x)$ is uncertain, it is clear that $z = T(x)$ is an uncertain nonlinear change of coordinates, hence $\delta(z,t)$ in the transformed system (12) is also unknown. The idea to deal with the uncertain term $\delta(z,t)$ is to lump it into a new state variable which can be interpreted as a new observable state. By an observer state, the dynamics of such state can be reconstructed from on-line measurements.

Now, let $\eta = \delta(z,t)$ be a state variable such that system (12) can be computed and can be interpreted as a new observable state as follows:

$$\begin{cases} \dot{z}_i = z_{i+1}, \quad 1 \leqslant i \leqslant \rho - 1, \\ \dot{z}_1 = \eta + u, \\ \dot{\eta} = \Xi(z,\eta,u,t), \end{cases} \tag{13}$$

here $\Xi(z,\eta,u,t) = \sum_{k=1}^{\rho-1} z_{k+1}\partial_k\delta(z,t) + (\eta+u)\partial_\rho\delta(z,t) + \partial_t\delta(z,t)$, with $\partial_k\delta(z,t) = \partial\delta(z,t)/\partial z_k$, $k = 1,2,\ldots,\rho$, $\partial_t\delta(z,t) = \partial\delta(z,t)/\partial t$, i.e., system (13) is dynamically equivalent to system (12). The manifold $\psi(z,\eta,t) = \eta - \delta(z,t)$ is, by definition, time-invariant, i.e., $\mathrm{d}\psi/\mathrm{d}t = 0$.

Then, let us consider the following linearizing control law to stabilize the uncertain system (13):

$$u = -\eta + \sum_{i=1}^{\rho} \theta^{(\rho-i+1)}\kappa_i z_i, \tag{14}$$

where $\theta \geqslant 0$ is a control gain introduced here to assign the convergence rate of the synchronization process and κ_i, $i = 1,2,\ldots,\rho$ are constant parameters which are computed from the following procedure. Eq. (13) under the controller (14) action results in the following closed-loop system:

$$\begin{cases} \dot{z} = \theta\Phi_\theta^{-1}A(\kappa)\Phi_\theta z, \\ \dot{\eta} = \Xi(z,\eta,u,t), \end{cases} \tag{15}$$

where the matrices $A(\kappa)$ and Φ_θ are given by

$$A(\kappa) = \begin{bmatrix} 0 & 1 & \cdots & 0 \\ \vdots & \vdots & \ddots & \vdots \\ 0 & 0 & \cdots & 1 \\ \kappa_1 & \kappa_2 & \cdots & \kappa_\rho \end{bmatrix} \quad \text{and} \quad \Phi_\theta = \begin{bmatrix} \theta^{-1} & 0 & \cdots & 0 \\ \vdots & \ddots & \ddots & \vdots \\ 0 & 0 & \ddots & 0 \\ 0 & 0 & \cdots & \theta^{-\rho} \end{bmatrix},$$

with Φ_θ^{-1} the inverse matrix of Φ_θ. Then κ_i, $i = 1,2,\ldots,\rho$ are chosen such that the matrix $A(\kappa)$ has all its eigenvalues at the open left-hand complex plane (i.e., all the roots of the polynomial $P_\rho(s) = s^\rho + \kappa_\rho s^{\rho-1} + \cdots + \kappa_2 s + \kappa_1$ have negative real parts).

Nevertheless, the linearizing feedback control law (14) is not physically realizable because of the uncertain state η. The problem can be addressed by using a high-gain observer [22].

$$\begin{cases} \dot{\hat{z}}_i = \hat{z}_{i+1} + \rho^i C_{\rho+1}^i(z_1 - \hat{z}_1), \quad 1 \leqslant i \leqslant \rho - 1, \\ \dot{\hat{z}}_1 = \hat{\eta} + u + L_0^\rho C_{\rho+1}^\rho(z_1 - \hat{z}_1), \\ \dot{\hat{\eta}} = L_0^{\rho+1}(z_1 - \hat{z}_1), \end{cases} \tag{16}$$

where $(\hat{z},\hat{\eta})$ are the estimated values of (z,η); $C_\rho^i = \frac{\rho!}{i!(\rho-i)}$ and $L_0 > 0$ represents a high-gain estimation parameter that can be interpreted as the uncertainties estimation rate and often be chosen as a constant. Note that the uncertain term $\Xi(z,\eta,u,t)$ has been neglected in the construction of the observer (16).

In our case, $\rho = 1$, then, the nonlinear controller becomes:

$$u = [-\hat{\eta} + \theta\kappa_1\hat{z}_1] \tag{17}$$

Consequently, implementing the controller (17) in the systems (6) and (7), we can get the following extended system that yield robust synchronization:

$$
\begin{cases}
\dot{x}_{1,\mathrm{M}} = \frac{1}{C_{\mathrm{mM}}}[I_{\mathrm{extM}} - \bar{g}_{\mathrm{NaM}} x_{2,\mathrm{M}}^3 h(x_{1,\mathrm{M}} - V_{\mathrm{NaM}} + V_{\mathrm{EM}}) - \bar{g}_{\mathrm{K}} x_{4,\mathrm{K}}^4 (V - V_{\mathrm{KM}} + V_{\mathrm{EM}}) \\
\qquad -\bar{g}_{\mathrm{lM}}(x_{1,\mathrm{M}} - V_{\mathrm{lM}} + V_{\mathrm{EM}})], \\
\dot{x}_{i,\mathrm{M}} = \alpha_y(x_{1,\mathrm{M}})(1 - x_{i,\mathrm{M}}) - \beta_y(x_{1,\mathrm{M}}) x_{i,\mathrm{M}}, \\
\dot{x}_{1,\mathrm{S}} = \frac{1}{C_{\mathrm{mS}}}[I_{\mathrm{extS}} - \bar{g}_{\mathrm{NaS}} x_{2,\mathrm{S}}^3 h(x_{1,\mathrm{S}} - V_{\mathrm{NaS}} + V_{\mathrm{EM}}) - \bar{g}_{\mathrm{K}} x_{4,\mathrm{S}}^4 (V - V_{\mathrm{KS}} + V_{\mathrm{EM}}) \\
\qquad -\bar{g}_{\mathrm{lS}}(x_{1,\mathrm{S}} - V_{\mathrm{lS}} + V_{\mathrm{EM}})] + (-\hat{\eta} + \kappa_1 \theta \hat{z}_1), \\
\dot{x}_{i,\mathrm{S}} = \alpha_y(x_{1,\mathrm{S}})(1 - x_{i,\mathrm{S}}) - \beta_y(x_{1,\mathrm{S}}) x_{i,\mathrm{S}}, \\
\dot{\hat{z}}_1 = \kappa_1 \theta \hat{z}_1 + L_0 C_2^1 ((x_{1,\mathrm{M}} - x_{2,\mathrm{S}}) - \hat{z}_1), \\
\dot{\hat{\eta}} = L_0^2 ((x_{1,\mathrm{M}} - x_{2,\mathrm{S}}) - \hat{z}_1), \\
y = m, h, n; \quad i = 2, 3, 4.
\end{cases} \tag{18}
$$

Now, let us carry out the numerical simulations to observe the synchronization of the HH neuronal systems. All the stimulations, the parameters and the initial conditions are the same as them in Section 4. The value of the control parameter $\kappa_1 = -1$, chosen for the polynomial $P(s)$ with its eigenvalues located at $s = -1$. The control gain and the high-gain estimation parameter were chosen to be $\theta = 2$ and $L_0 = 100$, respectively. The initial conditions of the observer (16) have been chosen as $(\hat{z}_1(0), \hat{\eta}(0)) = (1, 0)$. The modified controller is implemented at $t_0 = 200$ ms.

Fig. 12 shows the transition of the dynamical trajectory of slave neuron from chaotic to periodic under the controller (17). The synchronization error converges to zero after the controller (17) is applied, as shown in Fig. 13. And Fig. 14 is the V_{M}–V_{S} phase plane diagram of system (18), which shows the robust synchronization.

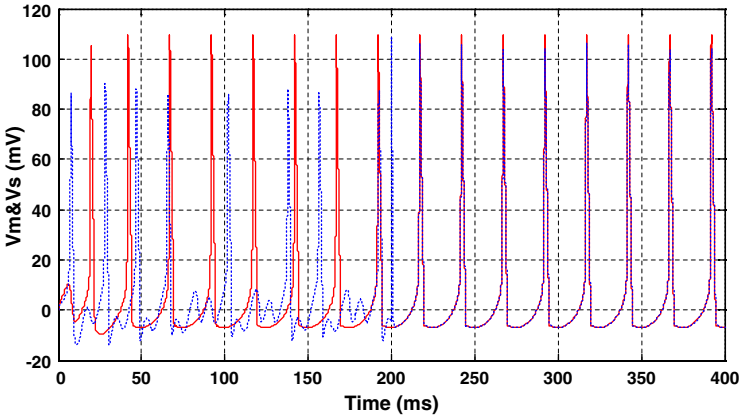

Fig. 12. Robust synchronized state of the action potentials under modified feedback control (17).

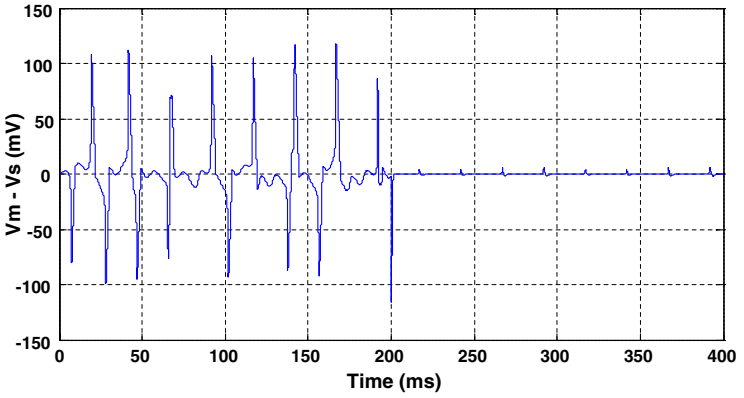

Fig. 13. Synchronization error of the system (18).

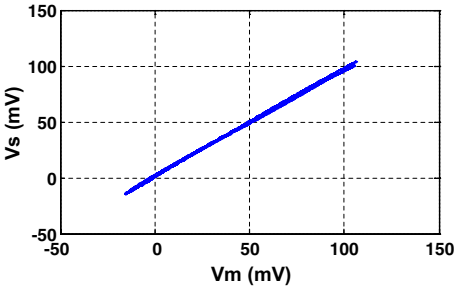

Fig. 14. Phase plane diagram of system (18).

6. Conclusions

In this paper, the dynamical behaviors of the individual modified HH model exposed to ELF electric field and control strategies of synchronization between two unidirectional coupled modified HH neurons are fully investigated.

Firstly, the dynamical behavior of the modified HH model under the ELF electric field is analyzed. The regular or chaotic state of the trans-membrane voltage is obtained, as shown in Figs. 3–5 and 6–8, respectively, the harmonious relationship between the external electric field and physiological parameters can be thoroughly investigated. Thus, the parameters of external electric field which is harmful to organisms could be defined so as to provide theoretical evidence for medical treatment and establishment of safety standard for electromagnetic exposure.

Secondly, we applied the nonlinear feedback control schemes to synchronize the modified HH neuronal systems using the analysis results of the first step. Under the feedback linearization scheme, exact synchronization can be achieved as shown in Figs. 9–11. However, because of immeasurable of some parameters, the first control law is not physically realizable. Thus, a modified feedback control law composed of a dynamic compensator and an uncertainties estimator has been implemented. The adaptive scheme leads to robust synchronization of the action potentials as shown in Figs. 12–14. Moreover, numerical simulations show that these two proposed control methods can effectively stabilize the chaotic trajectory of the slave system to periodic orbit.

Acknowledgement

The authors gratefully acknowledge the support of the NSFC (Nos. 50177023 and 50537030).

References

[1] Hodgkin AL, Huxley AF. Currents carried by sodium and potassium ions through the membrane of the giant axon of Loligo. J Physiol 1952;116:449–72.
[2] Hodgkin AL, Huxley AF. The dual effect of membrane potential on sodium conductance in the giant axon of Loligo. J Physiol 1952;116:497–506.
[3] Hodgkin AL, Huxley AF. A quantitative description of membrane and its application to conduction and excitation in nerve. J Physiol 1952;117:500–44.
[4] Hodgkin AL, Huxley AF. The components of membrane conductance in the giant axon of Loligo. J Physiol 1952;116:473–96.
[5] Wang Jiang, Che Yanqiu, Fei Xiangyang, Li Li. Multi-parameter Hopf bifurcation in Hodgkin–Huxley model exposed to ELF external electric field. Chaos, Solitons & Fractals 2005;26:1221–9.
[6] Kama H, Ying L. The dynamic principle of interaction between weak electromagnetic fields and living system—interference of electromagnetic waves in dynamic metabolism. Chin J Med Phys 1997;14(4).
[7] Stuchly MA, Dawson TW. Interaction of low-frequency electric and magnetic fields with the human body. Proc IEEE 2000;88:643–64.
[8] Blackman F. Influence of electromagnetic fields on the efflux of calcium ions from brain tissue in vitro: a three-model analysis consistent with the frequency response up to 510 Hz. Bioelectromagnetics 1988;9:215–327.
[9] Kotnik T, Miklavcic D. Second-order model of membrane electric field induced by alternating external electric fields. IEEE Trans Biomed Eng 2000;47:1974–81.
[10] Kotnik T, Miklavcic D. Theoretical evaluation of the distributed power dissipation in biological cells exposed to electric fields. Bioelectromagnetics 2000;21:385–94.

[11] Wiercigroch M, Krivtsov AM. Frictional chatter in orthogonal metal cutting. Philos Trans Roy Soc Lond A 2001;359:713–38.
[12] Ott E, Grebogi C, Yorke JA. Controlling chaos. Phys Rev Lett 1990;64:1196–9.
[13] Chen G, Moiola JL, Wang HO. Bifurcation: control and anticontrol. IEEE Trans Circ Syst I Newslett 1999;10:1–29.
[14] Fotsin Hilaire, Bowong Samuel, Daafouz Jamal. Adaptive synchronization of two chaotic systems consisting of modified Van der Pol–Duffing and Chua oscillators. Chaos, Solitons & Fractals 2005;26(1):215–29.
[15] Kyprianidis IM, Stouboulos IN. Chaotic synchronization of three coupled oscillators with ring connection. Chaos, Solitons & Fractals 2003;17(2–3):327–36.
[16] Zhou Shangbo, Liao Xiaofeng, Yu Juebang, Wong Kwok-Wo. Chaos and its synchronization in two-neuron systems with discrete delays. Chaos, Solitons & Fractals 2004;21(1):133–42.
[17] Shuai Jian-Wei, Durand Dominique M. Phase synchronizaiton in two coupled chaotic neurons. Phys Lett A 1999;264:289–97.
[18] Cornejo-Pérez O, Femat R. Unidirectional synchronization of Hodgkin–Huxley neurons. Chaos, Solitons & Fractals 2005;25:43–53.
[19] Wang Chun-Chieh, Su Juhng-Perng. A new adaptive variable structure control for chaotic synchronization and secure communication. Chaos, Solitons & Fractals 2004;20(5):967–77.
[20] Chen SH, Lu J. Synchronization of an uncertain unified system via adaptive control. Chaos, Solitons & Fractals 2002;14:643–7.
[21] Tan X, Zhang J, Yang Y. Synchronizing chaotic systems using backstepping design. Chaos, Solitons & Fractals 2003;16:37–45.
[22] Bowong Samuel, Moukam Kakmeni FM. Synchronization of uncertain chaotic systems via backstepping approach. Chaos, Solitons & Fractals 2004;21:999–1011.
[23] Yassen MT. Chaos synchronization between two different chaotic systems using active control. Chaos, Solitons & Fractals 2005;23:131–40.
[24] Cao Jinde, Li HX, Ho Daniel WC. Synchronization criteria of Lur'e systems with time-delay feedback control. Chaos, Solitons & Fractals 2005;23:1285–98.
[25] Sprott JC. Chaos and time-series analysis. Oxford University Press; 2003.
[26] Wolf A, Swift JB, Swinney HL, Vastano JA. Determining Lyapunov exponents from a time series. Physica D 1984;16:285–317.
[27] Femat R, Alvarez-Ramírez J, Fernández-Anaya G. Adaptive synchronization of high-order chaotic systems: a feedback with low-order parametrization. Physica D 2000;139:231.
[28] Femat R, Solís-Perales G. On the chaos synchronization phenomena. Phys Lett A 1999;262:50.
[29] Isidori. Nonlinear control systems. London, UK: Springer-Verlag; 1995.